

Anisotropy of strain and crystal deformations of partially relaxed InGaN layers grown on misoriented (0001)-GaN substrates

J. Moneta¹, M. Kryśko¹, J. Z. Domagala², E. Grzanka¹, G. Muziol¹, M. Siekacz¹, M. Leszczyński¹ and J. Smalc-Koziorowska¹

¹ Institute of High Pressure Physics, Polish Academy of Sciences, Sokolowska 29/37, 01-142 Warsaw, Poland

² Institute of Physics, Polish Academy of Sciences, Aleja Lotników 32/46, 02-668 Warsaw, Poland

Abstract

Strain relaxation of thick InGaN layers was studied in order to develop technology of InGaN templates for deposition of InGaN Quantum Wells (QWs) and InGaN layers of high-In-content. In this paper, we show that InGaN layers grown on misoriented (0001)-GaN substrates relax by preferential activation of certain glide planes for misfit dislocation formation. Substrate misorientation changes resolved shear stresses, affecting the distribution of misfit dislocations within each dislocation set. We demonstrate that this mechanism leads to an anisotropic strain as well as a tilt of the InGaN layer with respect to the GaN substrate. It appears that these phenomena are more pronounced in structures grown on substrates misoriented toward $\langle 11\bar{2}0 \rangle$ direction than corresponding structures with $\langle \bar{1}100 \rangle$ misorientation. These features would influence the properties of the overgrown InGaN QWs and should be taken into consideration during designing structures grown on relaxed InGaN templates. We reveal that the lattice of partially relaxed InGaN has a triclinic deformation, thus requiring advanced XRD analysis. The presentation of just a single asymmetric reciprocal space map commonly practiced in the literature can lead to misleading information regarding the relaxation state of partially relaxed wurtzite structures.

1. Introduction

III-nitrides: AlN, GaN and InN and their alloys have gained enormous importance in the fabrication of optoelectronic devices. Alloying of these compounds should enable a band gap engineering and color change of the emission wave in the range from deep ultraviolet 6.25 eV for AlN, through 3.51 eV for GaN, to infrared 0.78 eV for InN. The visible spectral range can be covered by the construction of devices based on the InGaN active layer. Commercially available blue and green light emitters are based on InGaN layers with an In-content of up to 30%. Higher In-content layers are desired for the further development of red color nitride-based devices, however, the growth of such layers remains challenging. Low growth temperatures are required, but low adatom mobility makes it difficult to achieve a good structural quality.[1] In addition, the large lattice mismatch between GaN and InN (11%) leads to strain-related problems such as formation of structural defects and composition pulling effect.[2-7] Theoretical calculations by Lymperakis et al.[8] showed fundamental limits close to 25% for In incorporation in InGaN layers grown coherently on the GaN substrate. To overcome these difficulties and to obtain high quality layers with higher In content, the idea of using relaxed InGaN layers as pseudo-substrates for the growth of InGaN-based devices has emerged in recent years.[9-16] Plastically relaxed $\text{In}_x\text{Ga}_{1-x}\text{N}$ (InGaN) layers deposited on GaN[2,14] or AlN[17] substrates exhibit a relatively low degree of plastic relaxation (generally less than 50%) even at high thicknesses. Although InGaN quantum wells with up to 30% In content grown on GaN substrates have been reported, the maximum In content in thick layers of reasonable structural quality does not exceed 20%. At higher In contents or higher degrees of relaxation, the layers exhibit dislocation densities above 10^{10} cm^{-2} and/or high densities of basal plane stacking faults.[2,14,17,18] Overcoming the current lack of plastically relaxed $\text{In}_x\text{Ga}_{1-x}\text{N}$ layers suitable as substrates requires a deeper understanding of the strain relaxation processes. Further strain engineering is essential to obtain InGaN templates of high structural quality with significant lattice parameter enlargement.

Misoriented substrates (also called miscut substrates) are typically used to promote the step-flow growth mode desired for the epitaxy of the highest quality layers. Misorientation is a configuration in which the crystallographic planes of the chosen substrate orientation are not exactly parallel to the surface, but are slightly tilted to expose surface steps (Fig. 1(a)). It can be introduced by mechanical polishing or locally by photolithography and etching[19]. Substrate misorientation influences various properties of the epitaxial layers such as morphology, atom incorporation, leads to unit cell deformation and affects strain relaxation

processes. It has been shown that GaN substrate misorientation between 0.5° and 1° allows to obtain surfaces with the smallest roughness with atomic steps in the case of InGaN growth. However, GaN substrate misorientation decreases the incorporation of indium into InGaN layers. [19] The presence of atomic steps at substrate surface introduced by the misorientation leads to elastic relaxation of the epitaxial layer and introduces crystallographic tilt as it was described by Nagai's model [20]. Such a layer tilt with respect to the substrate (0002) planes (*c*-planes) has also been reported for coherent InGaN layers [21]. In addition, the elastic relaxation at the substrate steps also leads to the inclination between the *c*-axis and the normal to the *c*-planes of InGaN lattice as shown by Kryško et al. [22] Similar lattice deformations have also been reported for cubic heterostructures, e.g. AlGaAs/GaAs [23].

Substrate misorientation also induces stress asymmetry that influences strain relaxation processes, including dislocation formation. It has been reported for epitaxial systems crystallizing in cubic structures, like InGaAs/GaAs [24,25] or SiGe/Si [26,27], that the imbalance in dislocation generation in various dislocation sets may occur as a result of the substrate misorientation. The Burgers vector of a misfit dislocation must contain the in-plane component which compensates differences in in-plane lattice parameters and directly realizes strain relaxation. However, such a misfit dislocation may also contain the out-of-plane component of the Burgers vector, then it acts as an additional atomic step and also introduces local tilt of the layer [28]. The macroscopic tilt introduced by a presence of misfit dislocations increases if there is a preferential formation of dislocations with a specific out-of-plane component. Such a tilt introduced by preferential dislocation formation has been observed in epitaxial systems crystallizing in cubic structures [27-29] as well as in semipolar relaxed nitride structures where only the $\langle 1\bar{2}10 \rangle (0001)$ slip system is active [30].

The aim of this work is to investigate how the (0001) GaN substrate misorientation (azimuth and miscut angle) influences the plastic relaxation and structural properties of InGaN layers. We show that the relaxation of InGaN layers deposited on misoriented substrates leads to anisotropic strain and that these InGaN layers exhibit a layer-to-substrate tilt that affects the final template misorientation. The triclinic deformation of the InGaN unit cell should be taken into account when studying relaxed InGaN layers using X-ray diffraction. The approximation of hexagonal symmetry applied to partially relaxed wurtzite layers grown on the miscut substrates leads to large errors in the estimated degree of relaxation.

2. Background

2.1. Tilt of the coherently strained InGaN layers

Crystallographic tilt is a common feature of many types of mismatched epitaxial layers. Elastic relaxation that occurs at atomic steps introduced by misorientation of the substrate leads to distortion of the lattice of the epitaxial layer (Fig. 1). Two effects can be distinguished: (i) layer-to-substrate tilt κ (called Nagai's tilt) and (ii) monoclinic deformation of the layer lattice, i.e., the inclination (tilt τ) between the **c**-axis and the normal to the **c**-planes of the layer lattice. Both tilts have a common origin and usually coexist. The tilt κ describes the relationship between the layer lattice and the substrate lattice, while the tilt τ refers to the deformation of the layer lattice itself. Both effects have been reported for coherent InGaN layers with respect to the underlying GaN [21,22].

Following the Nagai's model, the tilt of the heteroepitaxial coherent layer with respect to the substrate can be estimated as: $\tan\kappa = -(\frac{c_{\text{layer}} - c_{\text{substrate}}}{c_{\text{substrate}}})\tan\xi$, where c_{layer} , $c_{\text{substrate}}$ are out-of-plane lattice parameters and ξ is a substrate misorientation angle. It does not depend on the layer thickness. For example, the tilt of fully coherent $\text{In}_{0.2}\text{Ga}_{0.8}\text{N}$ with respect to 0.8° **m**-misoriented GaN (toward $\langle\bar{1}100\rangle$) is expected to be about 0.016° .

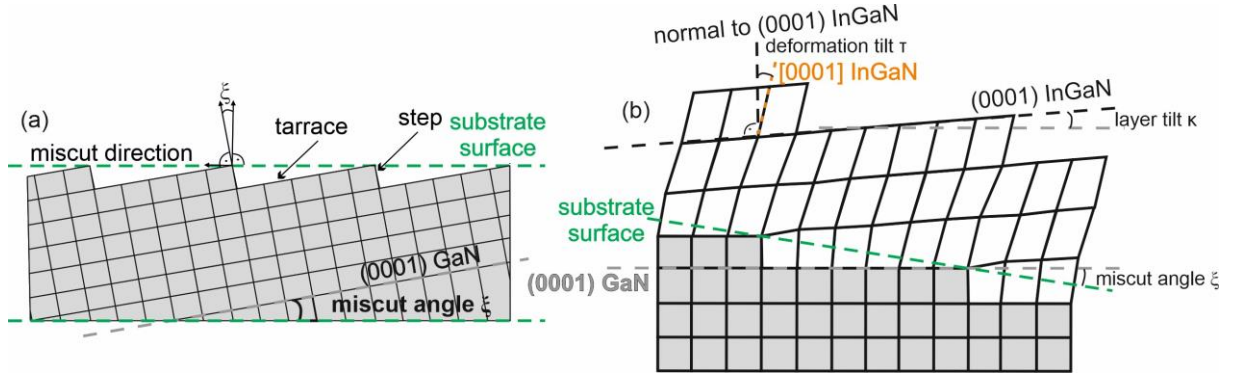


Fig. 1. Schematic illustration of (a) misoriented substrate and (b) heteroepitaxial coherent layer with lattice parameter $c_{\text{layer}} > c_{\text{substrate}}$. Deformation of the layer lattice occurs due to elastic strain relaxation at atomic steps: the layer is tilted with respect to the substrate (tilt κ between the **c**-planes of the layer and the substrate) and there is monoclinic distortion of the layer (tilt τ between the **c**-axis and the normal to the **c**-planes of the layer).

2.2. Introduction of misfit dislocations into a layer grown on misoriented substrate

During the epitaxial growth of materials with the same crystallographic structure, the lattice mismatch between the layer and the substrate leads to two phenomena: deformation of the layer lattice (elastic strain is observed) and, under favourable conditions, additional formation of linear defects. The dislocations store energy and generate a strain field.. The part of the mismatch accommodated by misfit dislocations can be expressed using elasticity theory. Coherent epitaxial layers are under biaxial stress:

$$[\sigma] = \begin{bmatrix} \sigma_{xx} & 0 & 0 \\ 0 & \sigma_{yy} & 0 \\ 0 & 0 & 0 \end{bmatrix}$$

(in the coordinate system related to the interface ((x, y, z), Fig. 2)). The wurtzite layer coherently grown on the (0001)-oriented substrate experiences an in-plane strain equal to the lattice mismatch:

$$\varepsilon_{xx} = \varepsilon_{yy} = f, \text{ where } f = \frac{a_{\text{substrate}} - a_{\text{layer}}}{a_{\text{layer}}}$$

and then an equibiaxial stress state:

$$\sigma_{xx} = \sigma_{yy} = \sigma = \frac{2(1-\nu)}{2-\nu} \varepsilon_{xx} \cdot [3I]$$

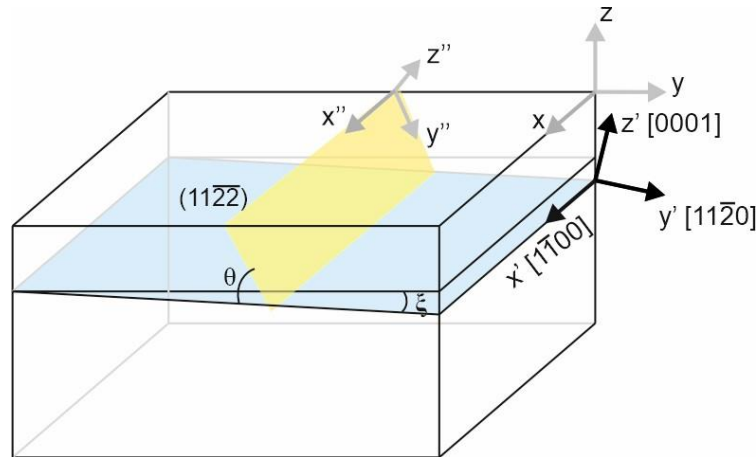


Fig. 2. Scheme of the wurtzite layer grown on the misoriented substrate. The coordinate systems used in the work are indicated: (x, y, z) related to the interface (surface), (x', y', z') related to the (0001) plane, (x'', y'', z'') related to the slip plane. The (0001) basal plane and the (11 $\bar{2}\bar{2}$) slip plane are marked in blue and yellow, respectively.

The general case of strain and stress acting in wurtzite layers grown on substrates with surface normal tilted away from the [0001] direction was studied by Romanov et al.[32,33]. The authors have studied structures in non-polar and semi-polar orientations, i.e., they have analyzed the full range of inclination angle ξ from 0° to 90° . In our work, we are analyzing layers grown on substrates misoriented only up to $\xi = 1.42^\circ$, so the stress is still close to the equibiaxial state.

The driving force behind the formation of misfit dislocations is the shear stress acting on the glide plane where movement occurs. Slip systems with higher resolved shear stresses experience a lower activation energy for dislocation nucleation and a higher glide velocity thus are therefore expected to dominate in the misfit dislocation formation process [24]. The glide geometry of the hexagonal crystal lattice is complex: three types of Burgers vectors ($\frac{1}{3}\langle 11\bar{2}0 \rangle$, $\frac{1}{3}\langle 11\bar{2}3 \rangle$, $\langle 0001 \rangle$) and at least five different types of glide planes ($\{0001\}$, $\{1\bar{1}00\}$, $\{11\bar{2}0\}$, $\{11\bar{2}2\}$, $\{1\bar{1}01\}$). For (0001)-oriented $\text{In}_x\text{Ga}_{1-x}\text{N}$ films, the easy slip systems of the hexagonal lattice ($\frac{1}{3}\langle 11\bar{2}0 \rangle\{0001\}$, $\frac{1}{3}\langle 11\bar{2}0 \rangle\{1\bar{1}00\}$) are usually inactive due to the lack of resolved shear stresses.[34] Activation of the slip systems on pyramidal planes in such oriented layers ($\frac{1}{3}\langle 11\bar{2}3 \rangle\{11\bar{2}2\}$, $\frac{1}{3}\langle 11\bar{2}3 \rangle\{1\bar{1}01\}$) requires high energies and has been observed only in high quality layers, without other structural defects that can hinder the formation and propagation of $1/3\langle 11\bar{2}3 \rangle$ defects. [34-36] The observed misfit dislocations with $\frac{1}{3}\langle 11\bar{2}3 \rangle$ Burgers vector, i.e., so-called **(a+c)** dislocations form a trigonal network along $\langle 1\bar{1}00 \rangle$ directions at the InGaN/GaN interface (Fig. 3(a)). The alignment of misfit dislocations along $\langle 1\bar{1}00 \rangle$ directions suggests dislocation nucleation and glide on the $\{11\bar{2}2\}$ slip planes (Fig. 3(b)). There are six $\{11\bar{2}2\}$ crystallographic planes in the wurtzite structure accessible for nucleation and glide of **(a+c)** dislocations. The planes can be grouped into three pairs of mirrored $\{11\bar{2}2\}$ planes e.g., the $(1\bar{2}12)$ and the $(1\bar{2}1\bar{2})$ planes. Glide of a misfit dislocation half-loop on each of the mirror pairs results in one set of parallel misfit dislocations lying along the respective $\langle 1\bar{1}00 \rangle$ direction (Fig. 3(a)). Owing to the symmetry of the crystallographic system, the specific dislocation lying in a particular $\langle 1\bar{1}00 \rangle$ direction can have one of four possible Burgers vectors (Table 1). To relieve the misfit strain, all dislocations belonging to one set should have the same **a**-component. Dislocations from the common set may differ only in the **c**-component depending on the chosen mirror plane (Fig. 3(b)).

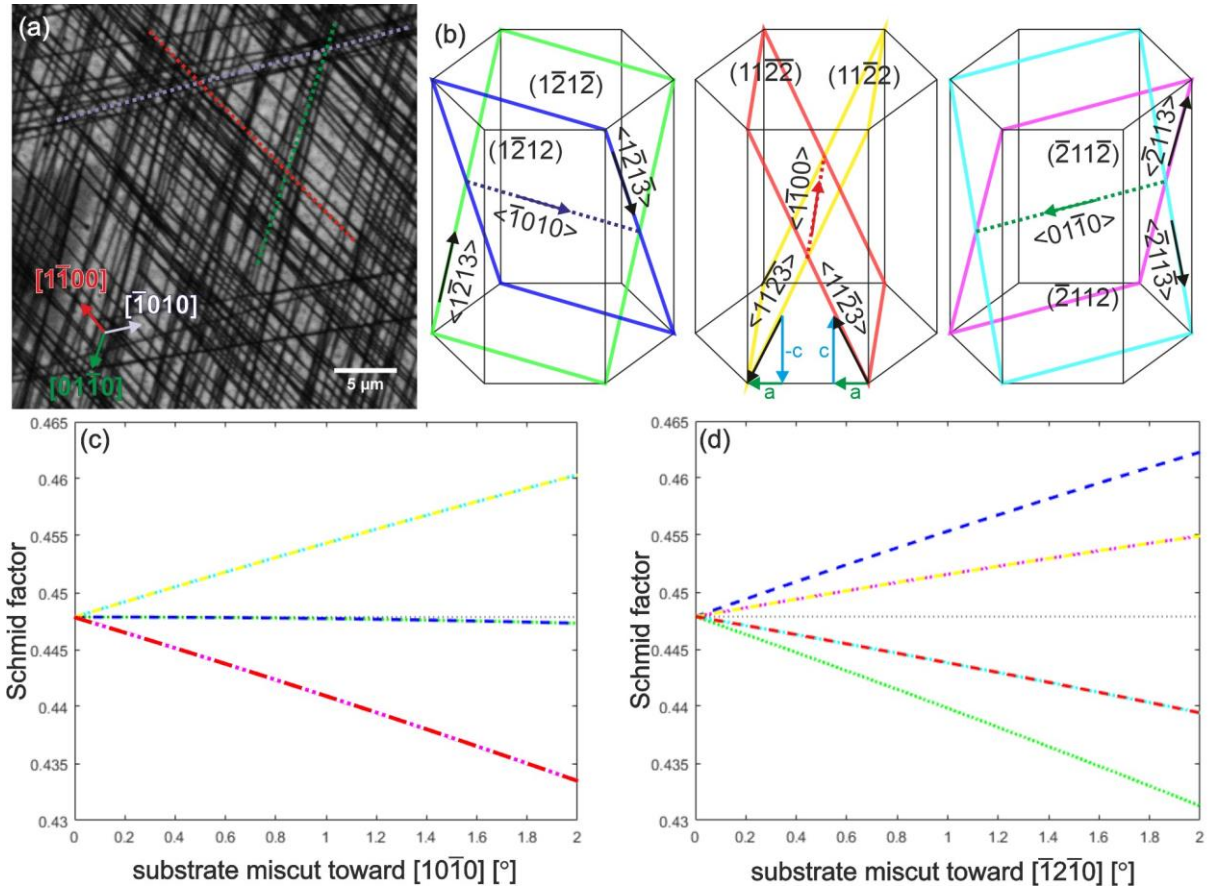


Fig. 3. (a) CL planar view image of a 50 nm thick $\text{In}_{0.2}\text{Ga}_{0.8}\text{N}$ layer. Misfit dislocations are visible as dark lines. The colors of the lines indicate the respective $\langle 1\bar{1}00 \rangle$ directions. (b) Schematic drawing of the pairs of mirror-related $\{11\bar{2}2\}$ planes and the corresponding $\langle 1\bar{1}00 \rangle$ directions. In-plane ('a') and out-of-plane ('c') components of $\frac{1}{3}[11\bar{2}3]$ and $\frac{1}{3}[112\bar{3}]$ Burgers vectors are marked with green and blue arrows, respectively. (c) – (d) Plots of calculated Schmid factors for each slip system as a function of the substrate misorientation. The colors of the lines correspond to the respective color-coded slip systems as shown in (b). The black dotted line indicates the value of the Schmid factor for the perfectly (0001)-oriented substrate.

Table 1. $\{11\bar{2}2\}$ slip planes with their corresponding Burgers vectors and resulting directions of the misfit dislocation (MD) line on the (0001) plane.

Pyramidal plane	$(\bar{2}11\bar{2})$	(2112)	(1212)	$(\bar{1}212)$	(1122)	$(\bar{1}122)$
Burgers vector	$\pm\frac{1}{3}[\bar{2}113]$	$\pm\frac{1}{3}[211\bar{3}]$	$\pm\frac{1}{3}[1\bar{2}13]$	$\pm\frac{1}{3}[\bar{1}21\bar{3}]$	$\pm\frac{1}{3}[1123]$	$\pm\frac{1}{3}[\bar{1}12\bar{3}]$
MD line	$[01\bar{1}0]$		$[\bar{1}010]$		$[\bar{1}100]$	

To analyze dislocation formation, the stresses acting in each slip system need to be determined. We transformed the stress tensor from the coordinate system related to the interface $[\sigma]$ ((x, y, z), Fig. 2) into a coordinate system related to the slip system $[\sigma]''$ ((x'', y'', z''), Fig. 2) using transformation matrices defined in terms of Euler angles. The final transformation was achieved in two steps. First, the transformation $[\sigma]' = \mathbf{a}[\sigma]\mathbf{a}^T$ from the coordinate system related to the interface $[\sigma]$ ((x, y, z), Fig. 2) to a coordinate system related to the (0001) plane $[\sigma]'$ ((x', y', z'), Fig. 2) was performed with the transformation matrix \mathbf{a}_m or \mathbf{a}_a for $[10\bar{1}0]$ and $[\bar{1}2\bar{1}0]$ substrate misorientation, respectively:

$$\mathbf{a}_m = \begin{bmatrix} \cos\xi & 0 & \sin\xi \\ 0 & 1 & 0 \\ -\sin\xi & 0 & \cos\xi \end{bmatrix}, \mathbf{a}_a = \begin{bmatrix} 1 & 0 & 0 \\ 0 & \cos\xi & \sin\xi \\ 0 & -\sin\xi & \cos\xi \end{bmatrix},$$

where ξ is the misorientation angle of the substrate.

Next, the transformation $[\sigma]'' = \mathbf{b}[\sigma]'\mathbf{b}^T$ was done to find the stress tensor in each slip system $[\sigma]''$ ((x'', y'', z''), Fig. 2). The transformation matrices \mathbf{b} for each slip system were defined by using (i) rotation by an angle of ψ around the z'-axis, (ii) rotation by an angle of θ around the x'-axis and (iii) rotation by an angle of φ around the z''-axis (Fig. 2):

$$\mathbf{b} = \begin{bmatrix} \cos\psi & \sin\psi & 0 \\ -\sin\psi & \cos\psi & 0 \\ 0 & 0 & 1 \end{bmatrix} \begin{bmatrix} 1 & 0 & 0 \\ 0 & \cos\theta & \sin\theta \\ 0 & -\sin\theta & \cos\theta \end{bmatrix} \begin{bmatrix} \cos\varphi & \sin\varphi & 0 \\ -\sin\varphi & \cos\varphi & 0 \\ 0 & 0 & 1 \end{bmatrix}.$$

In such coordinate system, the σ_{23}'' stress component of the $[\sigma]''$ matrix is significant for dislocation nucleation and glide. In further analysis, we considered the Schmid factors of the respective slip systems. The Schmid factor m is a parameter describing a ratio between the resolved shear stress acting in the given slip system σ_{23}'' and the interfacial normal stress σ : $m = \frac{\sigma_{23}''}{\sigma}$. We calculated Schmid factors for six $\langle 11\bar{2}3 \rangle \{11\bar{2}2\}$ slip systems for substrate misorientations toward $\langle \bar{1}100 \rangle$ and $\langle \bar{1}\bar{1}20 \rangle$ directions. The results as a function of substrate misorientation are presented in Figs 3(c)-(d). According to the Schmid factor model, slip systems with the highest Schmid factors are favored for the introduction of misfit dislocations. For no substrate misorientation the Schmid factor of each $\langle 11\bar{2}3 \rangle \{11\bar{2}2\}$ slip system is $m=0.4479$.

In the case of substrate misorientation toward $[\bar{1}010]$ (Fig. 3(c)), two sets of misfit dislocations along the $[0\bar{1}10]$ and $[\bar{1}100]$ directions are expected to dominate, since dislocation formation is favored in the corresponding $\frac{1}{3}[\bar{2}11\bar{3}](\bar{2}112)$ (cyan in Fig. 3) and $\frac{1}{3}[11\bar{2}3](11\bar{2}2)$ (yellow in Fig.

3) slip systems. Respective mirror slip systems would be less active due to lower Schmid factors than for the non-misoriented case. Misfit dislocations in the third set, along $[\bar{1}010]$ direction, parallel to the substrate miscut, could be generated equally in both $\frac{1}{3}[1\bar{2}13](1\bar{2}1\bar{2})$ (green in Fig. 3) and $\frac{1}{3}[1\bar{2}1\bar{3}](1\bar{2}12)$ (blue in Fig. 3) mirror slip systems, but with lower nucleation rate due to higher activation energy (lower Schmid factor, close to non-misoriented case).

In turn, substrates misoriented toward **a**-direction would result in a different dislocation distribution. In the case of substrate misorientation toward $[\bar{1}2\bar{1}0]$ (Fig. 3(d)), one set of misfit dislocations along the $[\bar{1}010]$ direction, perpendicular to the substrate miscut, is favored by the highest Schmid factor for the $\frac{1}{3}[1\bar{2}1\bar{3}](1\bar{2}12)$ slip system (blue in Fig. 3). In two other dislocation sets, i.e., $[0\bar{1}10]$ and $[\bar{1}100]$ directions, the $\frac{1}{3}[\bar{2}113](\bar{2}11\bar{2})$ (magenta in Fig. 3) and $\frac{1}{3}[112\bar{3}](11\bar{2}2)$ (yellow in Fig. 3) slip systems experience higher resolved shear stresses than the corresponding mirror planes.

2.3. Strain state in a layer with irregular net of misfit dislocations

If there is no GaN substrate misorientation, all $\langle 11\bar{2}3 \rangle \{ 11\bar{2}2 \}$ slip systems in the InGaN epilayer experience the same resolved shear stress, resulting in a regular trigonal dislocation network with the same dislocation density in each set as shown in Fig. 4(a). However, introducing the substrate misorientation changes the angles between the interface and each of the slip planes, thus modifying the resolved shear stresses in each of the slip systems, as it was discussed in the section 2.2. Schemes of dislocation networks expected for layers grown on misoriented substrates are shown in Figs 4(b)-(c). The irregularity of the dislocation densities in particular sets leads to an inequality of the strain tensor components. The strain relieved by a single array of misfit dislocations can be estimated as: $\delta = \frac{b_{\parallel}}{D}$, where b_{\parallel} is an in-plane edge component of the Burgers vector and D is a distance between dislocations. Relaxation is most efficient perpendicular to the dislocation line. To estimate the total strain accommodated by the trigonal dislocation network one needs to add the strain components of all dislocation sets. The tensorial nature of the strain must be considered. In the coordinate systems related to the dislocation lines (Fig. 4(a)), the particular tensors of relieved strain for each dislocation set can be assumed to

be $\delta = \begin{bmatrix} 0 & 0 & 0 \\ 0 & \delta & 0 \\ 0 & 0 & 0 \end{bmatrix}$. To add tensors one needs to transform them into the common coordinate

system. The sum gives the total strain accommodated by the regular trigonal dislocation

network (each dislocation set with $\delta = \frac{b_{\parallel}}{D}$): $\delta_{reg} = \begin{bmatrix} \frac{3}{2}\delta & 0 & 0 \\ 0 & \frac{3}{2}\delta & 0 \\ 0 & 0 & 0 \end{bmatrix}$. This ensures isotropic

relaxation.

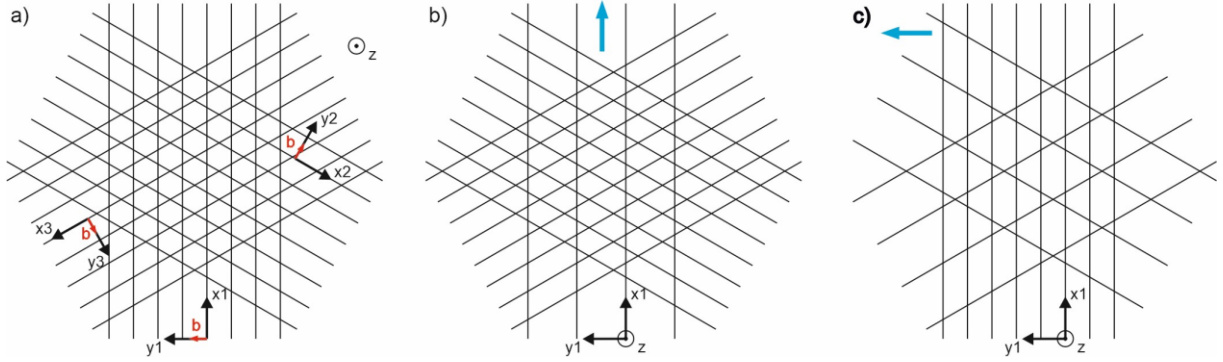


Fig. 4. Schemes of trigonal dislocation networks with a) equal dislocation density in each set, b) dislocation density twice lower in one set (corresponding to the dislocation distribution characteristic for InGaN layers grown on **m**-misoriented GaN substrates) and c) dislocation density twice lower in two sets (corresponding to the dislocation distribution characteristic for InGaN layers grown on **a**-misoriented GaN substrates). Coordinate systems related to each dislocation sets, to the set with the lowest dislocation density and to the set with the highest dislocation density are marked in (a), (b) and (c), respectively. The red arrows indicate Burgers vectors. The blue arrow marks the misorientation azimuth.

The situation changes for irregular dislocation networks. For illustration, we considered a dislocation network where the misfit relieved in two sets is equal to δ and in the third set is twice less (i.e., $\frac{1}{2}\delta$), which corresponds to the dislocation distribution characteristic of InGaN layers grown on **m**-misoriented GaN substrates (Fig. 4(b)) as well as a network where misfit relieved in one set is equal to δ and in two others is twice less ($\frac{1}{2}\delta$), which corresponds to the dislocation distribution characteristic of InGaN layers grown on **a**-misoriented GaN substrates

(Fig. 4(c)). Then, the total strain accommodated by the network is: $\delta_{tot}^m = \begin{bmatrix} \frac{3}{2}\delta & 0 & 0 \\ 0 & \delta & 0 \\ 0 & 0 & 0 \end{bmatrix}$ and

$$\delta_{tot}^a = \begin{bmatrix} \frac{5}{4}\delta & 0 & 0 \\ 0 & \frac{3}{4}\delta & 0 \\ 0 & 0 & 0 \end{bmatrix}, \text{ respectively.}$$

The lattice misfit is expressed by $f=\varepsilon+\delta$, [31] where ε is the residual elastic strain and δ is a part of the strain accommodated by misfit dislocations. Since $\delta_{xx} \neq \delta_{yy}$ and $\varepsilon = f - \delta$, then ε_{xx} is no longer equal to ε_{yy} . Thus, an irregular trigonal misfit dislocation network leads to anisotropic relaxation, i.e., the in-plane lattice parameter of the layer and hence the degree of relaxation will be different for different crystallographic directions.

3. Experimental

In_{0.2}Ga_{0.8}N layers were grown by Molecular Beam Epitaxy (MBE) at 630°C under metal-rich conditions. More details on the growth are provided in references [37,38]. Ammonothermal bulk GaN crystals of very low threading dislocation density (10^4 cm^{-2}) were used as substrates. The first set consists of two samples with 50 nm thick layer grown on substrates with 1° misorientation toward $\langle 11\bar{2}0 \rangle$ direction (**a**-misoriented substrate) and 0.81° misorientation toward $\langle \bar{1}100 \rangle$ direction (**m**-misoriented substrate). Two sets of 100 nm thick layers were deposited in one growth process on substrates with various miscut angles: 0.23°, 0.76° and 1.42° misorientation toward $\langle 11\bar{2}0 \rangle$ direction (set A) and 0.27°, 0.81° and 1.01° misorientation toward $\langle \bar{1}100 \rangle$ direction (set M). The substrate misorientation was determined by XRD measurements with an accuracy of $\pm 0.05^\circ$. The accuracy of the misorientation azimuth is of about a few degrees.

Structural and dislocation analysis was performed using transmission electron microscopy (TEM): FEI Tecnai G2 F20 S-TWIN operating at 200 kV and using cathodoluminescence imaging (CL) using a Hitachi SU-70 SEM Microscope with a CLUE Jobin Yvon system attached. Cross sectional and planar specimens for TEM analysis were prepared by mechanical polishing followed by ion milling.

Layer tilt, chemical composition and strain state were established using the High-Resolution X-ray Diffractometry (HRXRD) employing reciprocal space mapping (RSM). It is common practice to assume hexagonal symmetry in XRD strain analysis of epitaxial nitride layers. There

are then two unknown lattice parameters (a and c) and measurements of only two Bragg reflections are required. Typically, parameter c is found directly from a symmetric reflection (e.g., 0002 or 0004) and an asymmetric reflection is measured (e.g., $11\bar{2}4$ or $10\bar{1}5$) to determine parameter a , using the previously found value of c . Lattice parameter measurements provide information on the residual strain. Conventionally, the in-plane percent relaxation can be estimated by $R = \frac{a_L - a_S^0}{a_L^0 - a_S^0} \times 100$, where a_L is the measured in-plane lattice parameter of the layer, a_L^0 is the stress-free in-plane lattice parameter of the layer and a_S^0 is the in-plane lattice parameter of the substrate.

However, if the lattice distortion is present, more measurements are required. The hexagonal symmetry of strained epitaxial wurtzite layers can only be assumed at very low strain levels. The triclinic lattice deformation implies the need for detailed XRD measurements to find six unknowns: a , b and c lattice parameters and α , β and γ cell angles to accurately determine the chemical composition and the residual strain of the layer.

XRD measurements were performed using two high resolution diffractometers working with copper radiation ($\text{Cu}_{K\alpha 1}$, $\lambda=1.5406 \text{ \AA}$): Philips X'Pert MRD and Empyrean (Malvern Panalytical). Our approach consists of measuring six reciprocal space maps of $11\bar{2}4$ -type reflections and one 2θ - ω scan in tripple-axis mode of an 0002 symmetric reflection. Subsequent asymmetric maps were measured by rotating the sample clockwise every 60° around the normal to the surface. The position of an InGaN peak was determined as a mass center of the part of the peak that lies above the value $\frac{1}{2}I_{max}$, where I_{max} is the intensity of the highest point of the peak:

$$2\theta = \frac{\sum_n 2\theta_n (I_n - \frac{1}{2} I_{max})}{\sum_n (I_n - \frac{1}{2} I_{max})}.$$

Summation was performed over all points of the peak with intensity greater than $\frac{1}{2}I_{max}$. I_n and $2\theta_n$ are the intensity and 2θ of the n -th point, respectively.

We determined the parameters a , b , c , α , β and γ of the InGaN lattice by iteratively fitting the measured 2θ angles of one (0002) symmetric and six $\{11\bar{2}4\}$ asymmetric reflections to the positions of the theoretical unit cell. Details of the calculations are presented in the supplementary material. The direction of the found a parameter corresponds to the direction of the first measured asymmetric map. For the fully defined InGaN lattice, the tilt τ and its direction can be calculated from the lattice parameters using geometric relations. Next, both the strain and chemical composition must be determined together as both affect the lattice

parameters. With a fully defined lattice, the strain and the composition can be found by iterative fitting. However, in the intuitive coordinate system where the \mathbf{x} -axis is parallel to the \mathbf{a} -axis of the unit cell and the (\mathbf{x}, \mathbf{y}) plane is parallel to the axes \mathbf{a} and \mathbf{b} , shear strain ε_{xy} is not zero. Then, the degree of relaxation calculated with ε_{xx} and ε_{yy} components in such a coordinate system would be underestimated. To include the total strain in further considerations, we use tensor transformation to find the coordinate system $(\mathbf{x}', \mathbf{y}')$ in which the shear strain $\varepsilon_{x'y'}$ is zero ($\varepsilon_{x'y'}=0$), i.e., the principal coordinate system. Such defined \mathbf{x}' , \mathbf{y}' directions may deviate from the low indices crystallographic directions. By varying the indium content, $\varepsilon_{x'x'}$ and $\varepsilon_{y'y'}$ strain components and searching for the parameters with the best fit, the theoretical lattice can be found and compared with the lattice previously found from RSM measurements. Details of the calculations are presented in the supplementary material.

To illustrate a deviation from an in-plane symmetry, we define an anisotropy coefficient $A = \frac{\varepsilon_{y'y'}}{\varepsilon_{x'x'}}$, where $\varepsilon_{x'x'}$ and $\varepsilon_{y'y'}$ are calculated in-plane strain components defined in the coordinate system where $\varepsilon_{x'y'}=0$. Such a defined anisotropy coefficient A is equal to 1 for the isotropic layer and the deviation from this value increases with increasing anisotropy. We propose a way to express the degree of relaxation of partially relaxed wurtzite layers using the measured residual strain. The relaxation can then be described by the following two parameters: $R_{x'x'} = \frac{a_L^0 \varepsilon_{x'x'} + a_L^0 - a_S^0}{a_L^0 - a_S^0} \times 100$ and $R_{y'y'} = \frac{a_L^0 \varepsilon_{y'y'} + a_L^0 - a_S^0}{a_L^0 - a_S^0} \times 100$, where a_L^0 is the stress-free in-plane lattice parameter of the layer (the parameter of the unstrained cell calculated from Vegard's law for a given indium content), a_S^0 is the in-plane lattice parameter of the substrate and $\varepsilon_{x'x'}$ and $\varepsilon_{y'y'}$ are calculated in-plane strain components defined in the coordinate system for which $\varepsilon_{x'y'}=0$.

4. Results and discussion

TEM and CL analysis of InGaN layers reveal the trigonal network of $(\mathbf{a}+\mathbf{c})$ -type misfit dislocations aligned along $\langle \bar{1}100 \rangle$ directions for all analyzed samples. Figs 5(a)-(b) show CL images of 50 nm thick $\text{In}_{0.2}\text{Ga}_{0.8}\text{N}$ layers exhibiting an initial relaxation state. The dominance of either two sets of dislocations (Fig. 5(a)) or one set (Fig. 5(b)) for \mathbf{m} - and \mathbf{a} -misoriented substrates, respectively, is clearly visible. Fig. 5(c) shows a TEM image of 100 nm $\text{In}_{0.2}\text{Ga}_{0.8}\text{N}$ grown on \mathbf{m} -misoriented substrate. Dislocations are present in all three $\langle \bar{1}100 \rangle$ directions

indicating a higher degree of relaxation. However, it is still noticeable that the density of dislocations varies in different sets of dislocations.

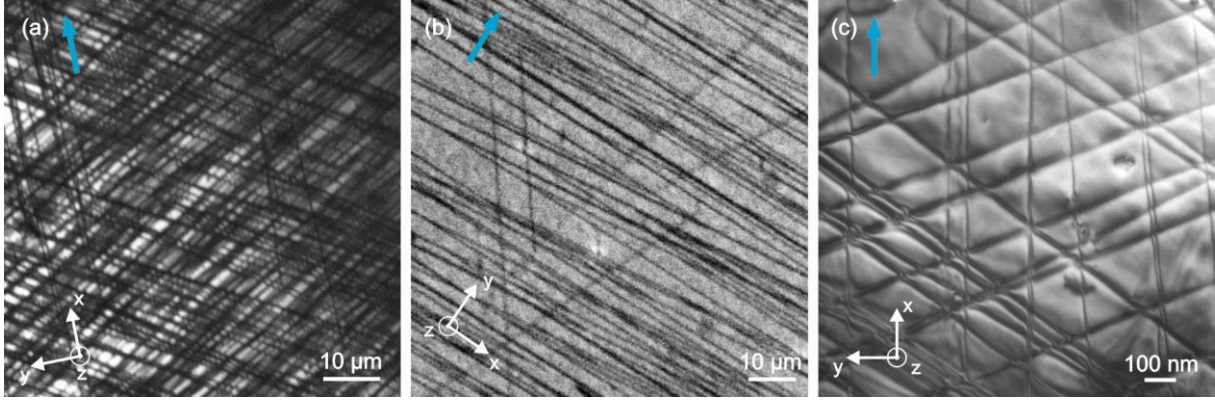


Fig. 5. CL planar view image of (a) 50 nm $\text{In}_{0.2}\text{Ga}_{0.8}\text{N}$ grown on **m**-misoriented substrate (0.81°) and (b) 50 nm $\text{In}_{0.2}\text{Ga}_{0.8}\text{N}$ grown on **a**-misoriented substrate (1°). (c) Plan-view bright-field TEM image of 100 nm $\text{In}_{0.2}\text{Ga}_{0.8}\text{N}$ grown on **m**-misoriented substrate (0.81°). Misfit dislocations are visible as dark lines. The blue arrow indicates the misorientation azimuth.

We estimated the degree of relaxation from the misfit dislocation density for 50 nm and 100 nm layers grown on **m**-misoriented substrate shown in Fig. 5. Average distances between dislocations in particular sets were calculated from CL images (image area of $10 \times 10 \mu\text{m}$) and TEM images (image area of $5 \times 5 \mu\text{m}$) (not shown here) for 50 nm and 100 nm thick layers, respectively. The strain relieved by a particular $\langle \bar{1}100 \rangle$ set was calculated as $\delta = \frac{b_{\parallel}}{D}$, where b_{\parallel} is an in-plane edge component of the Burgers vector and D is an average distance between dislocations. Next, all three δ components were transformed into the common (x, y) coordinate system related to the set with the lowest dislocation density, as shown in Fig. 5(a). The tensor of total strain accommodated by the network was defined in this coordinate system by adding the components of all dislocation sets. The δ_{xx} and δ_{yy} components of the tensor of total strain accommodated by the network were used to estimate the respective degrees of relaxation: $R_{ii} = \frac{\delta_{ii}}{f}$, where f is the misfit. We found 6%/4% and 30%/20% of relaxation in x/y directions for 50 nm and 100 nm thick $\text{In}_{0.2}\text{Ga}_{0.8}\text{N}$ layers, respectively.

Fig. 6 shows a high-resolution TEM image of two adjacent misfit dislocations with opposite **c**-components. The out-of-plane **c**-component of the dislocations introduces local tilt, visible as microscopic bending of the InGaN **c**-planes with respect to the GaN substrate. To relieve the

misfit strain, all dislocations belonging to one set should have the same in-plane **a**-component, however, no particular **c**-component is preferred in terms of strain relaxation. The out-of-plane **c**-component of their Burgers vectors, i.e., either “+**c**” or “-**c**”, depends on the slip plane chosen from the mirror-pair planes. The structural analysis shows that the majority of dislocations lying along the particular direction have the same Burgers vector, especially the same **c**-component, as we also reported elsewhere[36]. The resulting macroscopic tilt of the entire layer (the angle between the (0001) planes of the layer and the (0001) planes of the substrate) depends on the total sum of the **c**-components of the misfit dislocations.

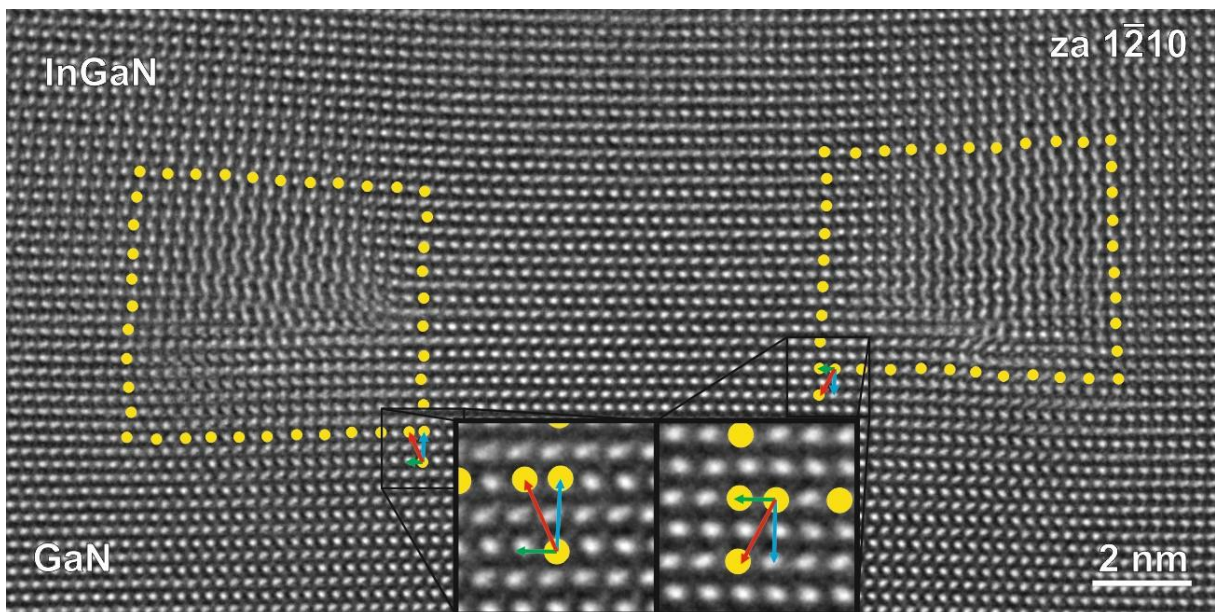


Fig. 6. High resolution TEM image taken along the $[1\bar{2}10]$ zone axis of two adjacent $(\mathbf{a}+\mathbf{c})$ -type misfit dislocations at the $\text{In}_{0.2}\text{Ga}_{0.8}\text{N}/\text{GaN}$ interface. The projection of the Burgers vector onto the image plane determined by the Burgers circuit is marked with red arrows. The in-plane components of the Burgers vector (marked with green arrows) are the same for both dislocations, while the out-of-plane components of the Burgers vector (marked with blue arrows) are opposite. The bending of the **c**-planes in the InGaN lattice is noticeable.

The XRD measurements were performed for 100 nm InGaN layers of the series with variable substrate misorientation (A and M sets). As an example, Fig. 7 shows reciprocal space maps of six $11\bar{2}4$ -type asymmetric reflections acquired for the InGaN layer deposited on 0.8°

m-misoriented GaN (M2). Table 2 shows the determined lattice parameters and Table 3 the calculated results of triclinic deformation, In content, strain analysis and layer tilt.

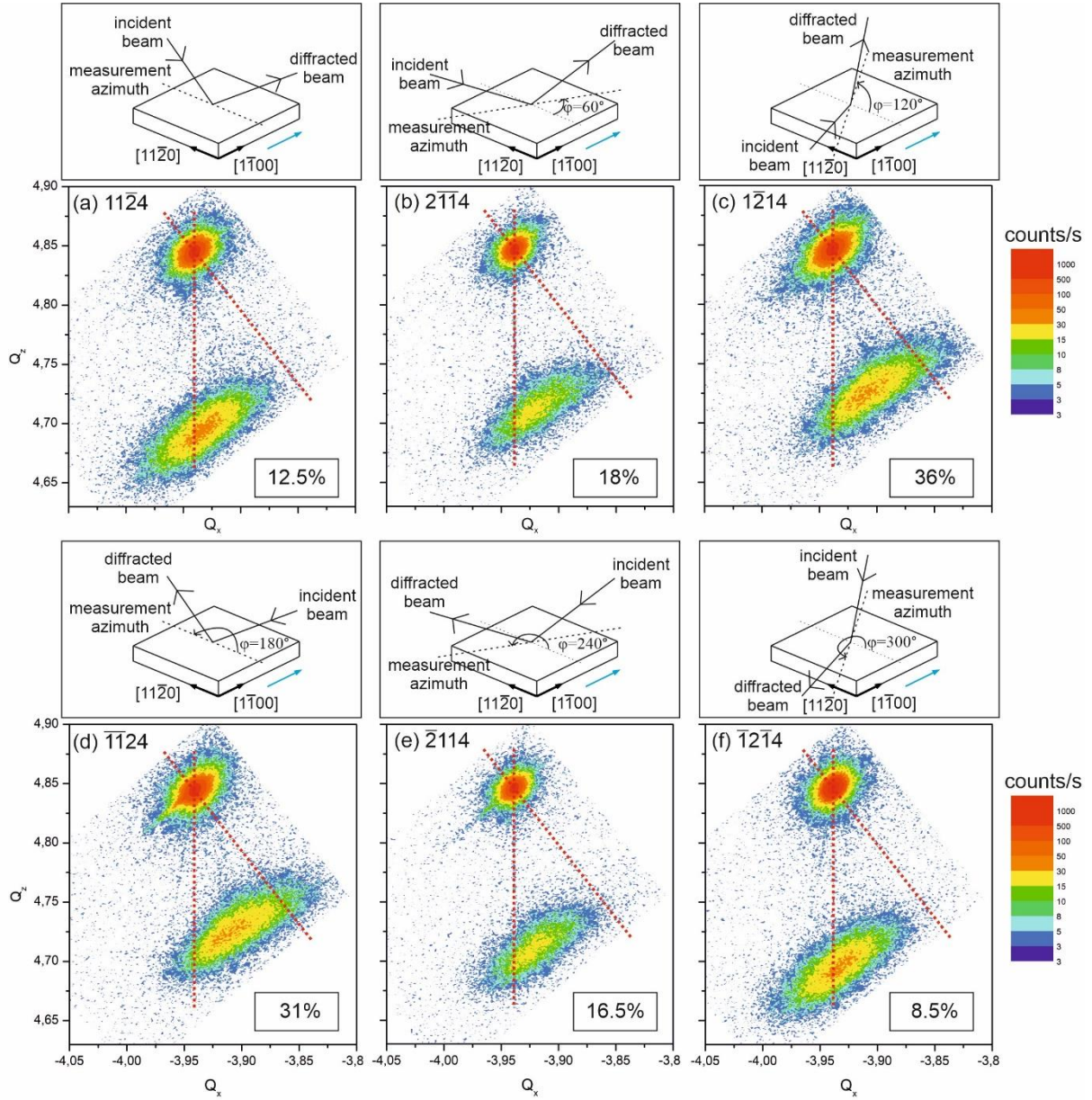


Fig. 7. Reciprocal space maps around asymmetric reflections a) $11\bar{2}4$, b) $2\bar{1}14$, c) $1\bar{2}14$, d) $\bar{1}\bar{1}24$, e) $\bar{2}114$, f) $\bar{1}\bar{2}\bar{1}4$ for 100 nm thick $\text{In}_{0.2}\text{Ga}_{0.8}\text{N}$ layer grown on 0.8° **m**-misoriented GaN (M2 sample) with measurement geometry. The blue arrow indicates the misorientation azimuth. The relaxation triangle is marked with red lines. The insets show the false degree of relaxation calculated for specific reflections assuming hexagonal symmetry (not triclinic one).

Table 2. XRD results of lattice parameters calculated for 100 nm InGaN layers.

Sample No. (substrate misorientation [°])	a [Å] ±0.0003	b [Å] ±0.0003	c [Å] ±0.0001	α [°] ±0.02	β [°] ±0.02	γ [°] ±0.02
A3 (1.42)	3.2021	3.2017	5.3253	90.08	90.07	119.84
A2 (0.76)	3.2057	3.2058	5.3323	90.04	90.03	119.92
A1 (0.23)	3.2066	3.2063	5.3345	90.03	90.01	119.99
M3 (1.01)	3.2042	3.2067	5.3279	90.10	89.90	120.05
M2 (0.81)	3.2073	3.2072	5.3321	90.08	89.92	120.03
M1 (0.27)	3.2049	3.2053	5.3331	90.03	89.97	120.01

Table 3. XRD results of In content, triclinic deformation, degree of relaxation and layer tilt for 100 nm InGaN layers.

Sample No. (substrate misorientation [°])	In content ±1 [%]	anisotropy coefficient A	deformation tilt τ ±0.02 [°]	Rx'x' ±3 [%]	Ry'y' ±3 [%]	layer tilt κ ±0.02 [°]
A3 (1.42)	18	0.80	0.14	16	33	0.27
A2 (0.76)	19	0.89	0.07	19	27	0.15
A1 (0.23)	19	0.99	0.03	21	21	0.02
M3 (1.01)	18	0.91	0.12	20	27	0.22
M2 (0.81)	19	0.96	0.09	21	24	0.17
M1 (0.27)	19	0.98	0.03	20	21	0.04

The indium content was found to be close to the nominal value in all samples. Decreasing indium content with increasing substrate miscut is a well-known phenomenon for InGaN layers grown by Metalorganic Vapor Phase Epitaxy in the step-flow growth mode[19]. However, Molecular Beam Epitaxy technique employs a much lower growth temperature and MBE-grown $\text{In}_{0.2}\text{Ga}_{0.8}\text{N}$ layers exhibit island formation on the (0001) surface which disrupts step-flow growth mode.[37] Then, it results in a weaker than expected dependence of indium incorporation as a function of substrate misorientation.[37,39]

The triclinic lattice distortion is notable for layers grown misoriented GaN substrates, although the differences in the lattice parameters are in the range of measurement accuracy. It was found that the tilt τ is opposite to the miscut direction and it increases with increasing misorientation, evidencing a more pronounced distortion. It is accompanied by a more pronounced in-plane anisotropy, which also increases with increasing misorientation: the anisotropy coefficient A

deviates more from the value of one. We found out that the observed relaxation mechanism is very sensitive to substrate misorientation. The lowest anisotropy occurs for the low miscut angles. Layers grown on 0.3° misoriented substrates show almost no anisotropy in the in-plane relaxation. Substrate misorientation of about 0.8° is large enough to introduce significant differences in degrees of relaxation. The largest difference is found for the A3 sample, where the relaxation changes from 16% to 33%, so almost twice, for orthogonal directions. Substrate misorientation toward **a**-direction introduces stronger anisotropy than the corresponding misorientation toward **m**-direction. Meanwhile, the average degree of relaxation for the corresponding layers is very similar. The degree of relaxation is comparable to the values obtained from the dislocation density indicating that the proposed $R_{x'x'}$ and $R_{y'y'}$ parameters are reliable. It is a common practice in the literature to present a reciprocal space map of only one asymmetric reflection of relaxed InGaN. The insets in Fig. 7 show the degree of relaxation calculated according to the standard procedure for all measured reflections with correction for layer tilt included. The values obtained with the hexagonal symmetry approximation differ significantly from each other and from the values calculated for the triclinic lattice. Since we have evidenced anisotropy in the dislocation distribution, we expect different degrees of relaxation in all three **a**-directions. However, the obtained values varied significantly even after 180° specimen rotation, e.g., from 8.5% to 36% for $\bar{1}\bar{2}14$ and $\bar{1}\bar{2}\bar{1}4$ reflections, respectively. In this case, equivalent results should be obtained since one is probing the same crystallographic direction. This makes such measurements unreliable. It appears that the hexagonal symmetry approximation is invalid and the standard procedure leads to significant errors in the study of relaxed wurtzite epitaxial layers on the miscut substrates. The presentation of just a single reciprocal space map can then give misleading information about the relaxation state.

The respective tilt κ between InGaN and GaN (0001)-planes was also measured by the XRD. For 50 nm thick layers, the dislocation density is too low to introduce a significant macroscopic tilt. It is about 0.02° , which is close to the estimated Nagai's tilt for this layer (0.016°). This layer is at the very beginning of the plastic relaxation process and it is nearly coherent with the substrate. The tilt increases as layer thickness and degree of relaxation increase. Table 3 presents results for 100 nm thick layers. The tilt κ increases with increasing miscut and becomes significant with respect to the substrate misorientations used, e.g., the tilt of the M2 layer is 0.17° with respect to a substrate misorientation of 0.81° . This is by an order of magnitude larger than the Nagai's tilt. It contributes to the total tilt, however, it decreases with increasing degree of plastic relaxation and tends to zero for fully relaxed layers. The measured tilt is mainly a

result of the preferential formation of misfit dislocations with a specific out-of-plane component due to the stress asymmetry introduced by the substrate misorientation. It was found that the layer tilt with respect to the substrate is opposite to the miscut direction, which leads to the decrease of the total structure misorientation.

Fig. 8 summarizes the observed lattice deformations: (i) a crystallographic tilt of the layer with respect to the substrate κ (Fig. 8(b)) and (ii) a triclinic distortion of the InGaN lattice which can be divided into 2 components: in-plane anisotropy manifested by the inequality of the **a** and **b** lattice parameters (Fig. 8(e)) and out-of-plane deformation described by the tilt τ between the **c**-axis and the normal to the **c**-planes of the InGaN lattice (Fig. 8(c)).

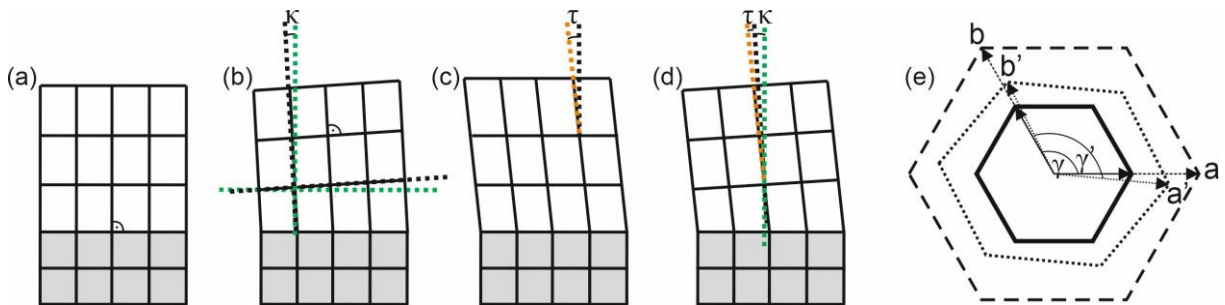


Fig. 8. Cross-section schematic illustration of (a) the tetragonally deformed layer, (b) the layer tilted with respect to the substrate (tilt κ between the layer and the substrate with undistorted layer lattice), (c) the distortion of the layer **c**-axis with respect to the layer **c**-planes (tilt τ between the **c**-axis and the normal to the layer **c**-planes) and (d) the presence of both κ and τ tilts like found in studied InGaN layers. (e) Schematic in-plane illustration of the anisotropy in the relaxed InGaN lattice. Solid and dashed lines correspond to wurtzite GaN and fully relaxed wurtzite InGaN respectively. Then the lattice parameters $a=b$ and $\gamma=120^\circ$ as well as a_{GaN} is parallel to a_{InGaN} . Dotted lines correspond to partially relaxed InGaN. According to XRD measurements $a' \neq b'$ and $\gamma' \neq 120^\circ$. The schemes show only the respective positions of the layer and substrate lattices. The interface structure is neglected.

The crystal curvature was measured in two orthogonal directions: toward and perpendicular to the substrate miscut. We found a small bowing radius (a few meters) of the InGaN layers while the underlying GaN substrates remain relatively flat. We continue investigation to understand this effect, which likely originates from the specificity of misfit dislocations and strong lattice deformation.

5. Conclusions

In the case of InGaN layers deposited on misoriented substrates, not all $\langle 11\bar{2}3 \rangle \{11\bar{2}2\}$ slip systems are equivalent for $(\mathbf{a}+\mathbf{c})$ -dislocation nucleation and glide which follows from the observation of different densities of misfit dislocations along different $\langle 1\bar{1}00 \rangle$ directions in CL and TEM studies and the differences in the density of dislocations with opposite \mathbf{c} -components. Both of these effects can be qualitatively explained by the Schmid factor model and attributed to the changes in resolved shear stresses induced by substrate misorientation. According to the model, the misorientation of a GaN substrate toward \mathbf{a} - or \mathbf{m} -directions in the wurtzite lattice result in the dominance of one or two sets of misfit dislocations, respectively. Such a mismatch in the dislocation distribution leads to strain anisotropy in the InGaN epitaxial layers, which is confirmed by our structural studies. As expected from the dislocation distribution model, it was found that higher misorientation decreases the energy for dislocation nucleation in some glide planes, while it has an opposite effect in others, leading to higher strain anisotropy. The layer tilt also increases as the substrate miscut increases due to enhanced imbalance in dislocation formation on the mirrored $\{11\bar{2}2\}$ planes. It is worth noting that the tilt of the layer with respect to the substrate reduces the initial substrate misorientation resulting in a different total misorientation of the final structure. Since substrate misorientation strongly affects the properties of InGaN layers[19], the InGaN tilt should also be considered in the design of such substrates for the potential application of relaxed InGaN as pseudo-substrates. Layers grown on 0.3° misoriented substrates show almost no anisotropy in the in-plane relaxation along with relatively small layer tilt, however, layers grown on 0.8° misoriented substrates exhibit significant lattice deformation.

We observed the discussed phenomena in a wide range of plastically relaxed InGaN layers grown by MBE or MOVPE techniques. The observed mechanism is universal, independent of the type of GaN substrate used and its threading dislocation density (TDD), such as bulk GaN substrates prepared by halide vapor phase epitaxy (TDD $\sim 10^6 \text{ cm}^{-2}$) or by ammonothermal growth (TDD $\sim 10^4 \text{ cm}^{-2}$) or on GaN/sapphire templates (TDD $\sim 10^8 \text{ cm}^{-2}$).

In summary, we have demonstrated that InGaN layers grown on misoriented substrates relax by preferential activation of certain glide planes for misfit dislocation formation. We observe two different aspects of preferential dislocation formation: (i) the preferential glide on one plane from mirror related pairs leading to the tilting of the layer with respect to the substrate and (ii)

the preferential formation of dislocations in particular $\langle \bar{1}100 \rangle$ sets leading to in-plane anisotropy of the layer. Such an imbalance in dislocation generation is the result of the GaN substrate misorientation, which changes the shear stresses acting in the respective glide planes, resulting in a different dislocation nucleation ratio in each dislocation set. Accordingly, the perfect wurtzite symmetry of the layer is no longer preserved and triclinic deformation of the lattice is observed. This implies the need for detailed XRD measurements of the strain state of the layer. The estimation of the degree of relaxation from the single asymmetric Bragg reflection, which is a common practice in the literature, can then lead to misleading conclusions. We observe substantial differences in the estimated relaxation state depending on the chosen $\{11\bar{2}4\}$ reflection. It appears that to properly determine the properties of relaxed InGaN by XRD measurements, it is necessary to include the triclinic distortion of the InGaN lattice. We defined the InGaN lattice by measuring the positions of a symmetric and all six $\{11\bar{2}4\}$ asymmetric reflections. We propose to describe the strain relaxation of anisotropic partially relaxed InGaN layers by two parameters of degree of relaxation: $R_{x'x'}$ and $R_{y'y'}$ defined by the measured residual strains in two orthogonal directions found in a coordinate system for which the in-plane shear strain is zero. Additionally, the tilt of the layer with respect to the substrate appears and changes the total misorientation of the final structure. These features would influence the properties of the layers deposited on such plastically relaxed InGaN. Thus, the development of structures grown on relaxed InGaN buffers should reckon these effects.

Acknowledgments

This work was funded in part National Science Center, Poland, project OPUS LAP 2020/39/I/ST5/03379 and by Deutsche Forschungsgemeinschaft, Germany, project 465219948. For the purpose of Open Access, the author has applied a CC-BY public copyright license to any Author Accepted Manuscript (AAM) version arising from this submission. This research was also supported by Project of National Science Center 2018/31/G/ST5/03765.

References

- [1] T. Matsuoka, T. Sasaki, and A. Katsui, "Growth and properties of a wide-gap semiconductor InGaN", *Optoelectronics Tokyo* **5**, 53 (1990).
- [2] C. Bazioti, E. Papadomanolaki, T. Kehagias, T. Walther, J. Smalc-Koziorowska, E. Pavlidou, P. Komninou, T. Karakostas, E. Iliopoulos, and G. P. Dimitrakopoulos, "Defects, strain relaxation, and

- compositional grading in high indium content InGaN epilayers grown by molecular beam epitaxy", *Journal of Applied Physics* **118**, 155301 (2015).
- [3] Z. Liliental-Weber, K. M. Yu, M. Hawkrige, S. Bedair, A. E. Berman, A. Emara, J. Domagala, and J. Bak-Misiuk, "Spontaneous stratification of InGaN layers and its influence on optical properties", *physica status solidi c* **6**, S433 (2009).
- [4] A. M. Fischer, Z. Wu, K. Sun, Q. Wei, Y. Huang, R. Senda, D. Iida, M. Iwaya, H. Amano, and F. A. Ponce, "Misfit strain relaxation by stacking fault generation in InGaN quantum wells grown on m-plane GaN", *Applied Physics Express* **2**, 0410021 (2009).
- [5] G. B. Stringfellow, "Microstructures produced during the epitaxial growth of InGaN alloys", *Journal of Crystal Growth* **312**, 735 (2010).
- [6] S. Pereira, M. R. Correia, E. Pereira, K. P. O'donnell, C. Trager-Cowan, F. Sweeney, and E. Alves, "Compositional pulling effects in $\text{In}_x\text{Ga}_{1-x}\text{N}/\text{GaN}$ layers: A combined depth-resolved cathodoluminescence and Rutherford backscattering/channeling study", *Physical Review B* **64**, 205311 (2001).
- [7] Z. Liliental-Weber, M. Benamara, J. Washburn, J. Z. Domagala, J. Bak-Misiuk, E. L. Piner, J. C. Roberts, and S. M. Bedair, "Relaxation of InGaN thin layers observed by X-ray and transmission electron microscopy studies", *Journal of Electronic Materials* **30**, 439 (2001).
- [8] L. Lymperakis, T. Schulz, C. Freysoldt, M. Anikeeva, Z. Chen, X. Zheng, B. Shen, C. Chä"Ze, M. Siekacz, X. Q. Wang, M. Albrecht, and J. Neugebauer, "Elastically frustrated rehybridization: Origin of chemical order and compositional limits in InGaN quantum wells", *Physical Review Materials* **2**, 011601 (2018).
- [9] A. Even, G. Laval, O. Ledoux, P. Ferret, D. Sotta, E. Guiot, F. Levy, I. C. Robin, and A. Dussaigne, "Enhanced In incorporation in full InGaN heterostructure grown on relaxed InGaN pseudo-substrate", *Applied Physics Letters* **110**, 262103 (2017).
- [10] A. Dussaigne, F. Barbier, B. Samuel, A. Even, R. Templier, F. Lévy, O. Ledoux, M. Rozhavskaia, and D. Sotta, "Strongly reduced V pit density on InGaNOS substrate by using InGaN/GaN superlattice", *Journal of Crystal Growth* **533**, 125481 (2020).
- [11] S. S. Pasayat, C. Gupta, Y. Wang, S. P. Denbaars, S. Nakamura, S. Keller, and U. K. Mishra, "Compliant Micron-Sized Patterned InGaN Pseudo-Substrates Utilizing Porous GaN", *Materials* **13**, 213 (2020).
- [12] C. Wurm, H. Collins, N. Hatui, W. Li, S. Pasayat, R. Hamwey, K. Sun, I. Sayed, K. Khan, E. Ahmadi, S. Keller, and U. Mishra, "Demonstration of device-quality 60% relaxed $\text{In}_{0.2}\text{Ga}_{0.8}\text{N}$ on porous GaN pseudo-substrates grown by PAMBE", *Journal of Applied Physics* **131**, 015701 (2022).
- [13] V. Rieni, J. Smith, N. Lim, H.-M. Chang, P. Chan, M. S. Wong, M. J. Gordon, S. P. Denbaars, and S. Nakamura, "Demonstration of III-Nitride Red LEDs on Si Substrates via Strain-Relaxed Template by InGaN Decomposition Layer", *Crystals* **12**, 1144 (2022).
- [14] K. Hestroffer, F. Wu, H. Li, C. Lund, S. Keller, J. S. Speck, and U. K. Mishra, "Relaxed c -plane InGaN layers for the growth of strain-reduced InGaN quantum wells", *Semiconductor Science and Technology* **30**, 105015 (2015).
- [15] M. Siekacz, P. Wolny, T. Ernst, E. Grzanka, G. Staszczak, T. Suski, A. Feduniewicz-Żmuda, M. Sawicka, J. Moneta, M. Anikeeva, T. Schulz, M. Albrecht, and C. Skierbiszewski, "Impact of the substrate lattice constant on the emission properties of InGaN/GaN short-period superlattices grown by plasma assisted MBE", *Superlattices and Microstructures* **133**, 106209 (2019).
- [16] T. Schulz, L. Lymperakis, M. Anikeeva, M. Siekacz, P. Wolny, T. Markurt, and M. Albrecht, "Influence of strain on the indium incorporation in (0001) GaN", *Physical Review Materials* **4**, 073404 (2020).
- [17] G. Dimitrakopoulos, C. Bazioti, E. Papadomanolaki, K. Filintoglou, M. Katsikini, J. Arvanitidis, and E. Iliopoulos, "Evolution of stratification in high-alloy content InGaN epilayers grown on (0001) AlN", *Materials Science and Technology* **34**, 1565 (2018).
- [18] S. Valdueza-Felip, E. Bellet-Amalric, A. Núñez-Cascajero, Y. Wang, M.-P. Chauvat, P. Ruterana, S. Pouget, K. Lorenz, E. Alves, and E. Monroy, "High In-content InGaN layers synthesized by

- plasma-assisted molecular-beam epitaxy: Growth conditions, strain relaxation, and In incorporation kinetics", *Journal of Applied Physics* **116**, 233504 (2014).
- [19] M. Sarzynski, M. Leszczynski, M. Krysko, J. Z. Domagała, R. Czernecki, and T. Suski, "Influence of GaN substrate off-cut on properties of InGaN and AlGaIn layers", *Crystal Research and Technology* **47**, 321 (2012).
- [20] H. Nagai, "Structure of vapor-deposited Ga_xIn_{1-x}As crystals", *Journal of Applied Physics* **45**, 3789 (1974).
- [21] M. Kryśko, J. Z. Domagała, R. Czernecki, M. Leszczynski, P. Perlin, T. Suski, S. Grzanka, G. Targowski, I. Grzegory, M. Boćkowski, and S. Porowski, "Tilt of InGaIn layers on miscut GaN substrates", *physica status solidi (RRL) – Rapid Research Letters* **4**, 142 (2010).
- [22] M. Krysko, J. Z. Domagała, R. Czernecki, and M. Leszczynski, "Triclinic deformation of InGaIn layers grown on vicinal surface of GaN (00.1) substrates", *Journal of Applied Physics* **114**, 113512 (2013).
- [23] A. Leiberich and J. Levkoff, "The crystal geometry of Al_xGa_{1-x}As grown by MOCVD on offcut GaAs (100) substrates", *Journal of Crystal Growth* **100**, 330 (1990).
- [24] R. S. Goldman, K. L. Kavanagh, H. H. Wieder, S. N. Ehrlich, and R. M. Feenstra, "Effects of GaAs substrate misorientation on strain relaxation in In_xGa_{1-x}As films and multilayers", *Journal of Applied Physics* **83**, 5137 (1998).
- [25] S. P. Edirisinghe, A. E. Staton-Bevan, and R. Grey, "Relaxation mechanisms in single In_xGa_{1-x}As epilayers grown on misoriented GaAs(111)B substrates", *Journal of Applied Physics* **82**, 4870 (1997).
- [26] F. K. Legoues, P. M. Mooney, and J. Tersoff, "Measurement of the activation barrier to nucleation of dislocations in thin films", *Physical Review Letters* **71**, 396 (1993).
- [27] F. K. Legoues, P. M. Mooney, and J. O. Chu, "Crystallographic tilting resulting from nucleation limited relaxation", *Applied Physics Letters* **62**, 140 (1993).
- [28] J. E. Ayers, S. K. Ghandhi, and L. J. Schowalter, "Crystallographic tilting of heteroepitaxial layers", *Journal of Crystal Growth* **113**, 430 (1991).
- [29] R. J. Sichel, A. Grigoriev, D.-H. Do, S.-H. Baek, H.-W. Jang, C. M. Folkman, C.-B. Eom, Z. Cai, and P. G. Evans, "Anisotropic relaxation and crystallographic tilt in BiFeO₃ on miscut SrTiO₃ (001)", *Applied Physics Letters* **96**, 051901 (2010).
- [30] E. C. Young, F. Wu, A. E. Romanov, A. Tyagi, C. S. Gallinat, S. P. Denbaars, S. Nakamura, and J. S. Speck, "Lattice tilt and misfit dislocations in (11-22) semipolar GaN heteroepitaxy", *Applied Physics Express* **3**, 011004 (2010).
- [31] J. P. Hirth and J. Lothe, "Theory of Dislocations", Krieger Publishing Company, 1982.
- [32] A. E. Romanov, T. J. Baker, S. Nakamura, J. S. Speck, and E. J. U. Group, "Strain-induced polarization in wurtzite III-nitride semipolar layers", *Journal of Applied Physics* **100** (2006).
- [33] A. M. Smirnov, A. V. Kremleva, S. S. Sharofidinov, and A. E. Romanov, "Misfit stress relaxation in wide bandgap semiconductor heterostructures with trigonal and hexagonal crystal structure", *Journal of Applied Physics* **131** (2022).
- [34] S. Srinivasan, L. Geng, R. Liu, F. A. Ponce, Y. Narukawa, and S. Tanaka, "Slip systems and misfit dislocations in InGaIn epilayers", *Applied Physics Letters* **83**, 5187 (2003).
- [35] M. Iwaya, T. Yamamoto, D. Iida, Y. Kondo, M. Sowa, H. Matsubara, K. Ishihara, T. Takeuchi, S. Kamiyama, and I. Akasaki, "Relationship between misfit-dislocation formation and initial threading-dislocation density in GaInN/GaN heterostructures", *Japanese Journal of Applied Physics* **54**, 115501 (2015).
- [36] J. Moneta, M. Siekacz, E. Grzanka, T. Schulz, T. Markurt, M. Albrecht, and J. Smalc-Koziorowska, "Peculiarities of plastic relaxation of (0001) InGaIn epilayers and their consequences for pseudo-substrate application", *Applied Physics Letters* **113**, 031904 (2018).
- [37] H. Turski, M. Siekacz, M. Sawicka, G. Cywinski, M. Krysko, S. Grzanka, J. Smalc-Koziorowska, I. Grzegory, S. Porowski, Z. R. Wasilewski, and C. Skierbiszewski, "Growth mechanism of InGaIn by plasma assisted molecular beam epitaxy", *Journal of Vacuum Science and Technology B: Microelectronics and Nanometer Structures* **29**, 03C136 (2011).

- [38] M. Siekacz, A. Feduniewicz-Zmuda, G. Cywinski, M. Krysko, I. Grzegory, S. Krukowski, K. E. Waldrip, W. Jantsch, Z. R. Wasilewski, S. Porowski, and C. Skierbiszewski, "Growth of InGaN and InGaN/InGaN quantum wells by plasma-assisted molecular beam epitaxy", *Journal of Crystal Growth* **310**, 3983 (2008).
- [39] M. Leszczynski, R. Czernecki, S. Krukowski, M. Krysko, G. Targowski, P. Prystawko, J. Plesiewicz, P. Perlin, and T. Suski, "Indium incorporation into InGaN and InAlN layers grown by metalorganic vapor phase epitaxy", *Journal of Crystal Growth* **318**, 496 (2011).

Supplementary material to:

Anisotropy of strain and crystal deformations of partially relaxed InGaN layers grown on misoriented (0001)-GaN substrates

J. Moneta¹, M. Kryśko¹, J. Z. Domagala², E. Grzanka¹, G. Muziol¹, M. Siekacz¹, M. Leszczyński¹ and J. Smalc-Koziorowska¹

¹ Institute of High Pressure Physics, Polish Academy of Sciences, Sokolowska 29/37, 01-142 Warsaw, Poland

² Institute of Physics, Polish Academy of Sciences, Aleja Lotników 32/46, 02-668 Warsaw, Poland

Calculations performed in the frame of XRD analysis

Partially relaxed InGaN layers on miscut substrates exhibit significant triclinic lattice deformation (Fig. S1). To accurately determine the chemical composition (indium content) and the residual strain of the layer, more XRD measurements is required than in the case of a strained layer deposited on on-axis substrate. Our approach consists of measuring of six reciprocal space maps of $11\bar{2}, 4$ -type reflections and one 2θ - ω scan in tripple-axis mode of a symmetric reflex, e.g., 0002. Subsequent asymmetric maps are measured by rotating the sample every 60 degrees around normal to the surface clockwise. We use the 2θ angles of the maxima of the layer peaks for these 6 asymmetric maps ($2\theta_{\text{asym}_1}, \dots, 2\theta_{\text{asym}_6}$) and for symmetric reflection ($2\theta_{\text{sym}}$).

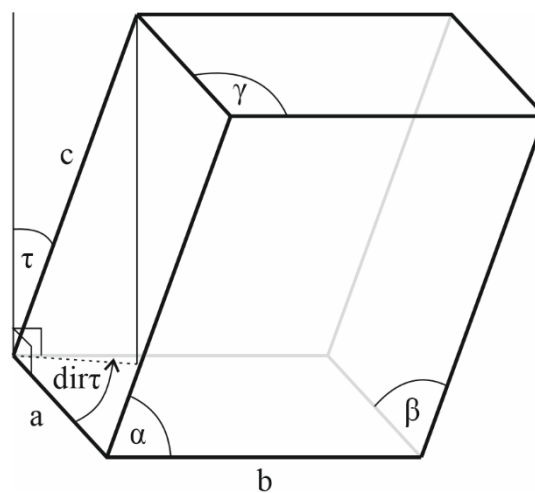


Fig. S1 Illustration of triclinic unit cell with marked $a, b, c, \alpha, \beta, \gamma$ lattice parameters and the tilt τ and its direction $\text{dir}\tau$.

We assume that the direction of the \mathbf{a} -axis of unit cell corresponds to the azimuthal direction of the first measured asymmetric map. We determine the parameters a , b , c , α , β and γ of the InGaN lattice (Fig. S1) by the iterative fitting of the theoretical values to the measured ones using the following method:

1. We determine parameter c from Bragg's condition for the symmetric reflection ($2\theta_{\text{sym}}$), taking into account the refractive correction.
2. We find the interplanar distances d_1 to d_6 from Bragg's condition for the angles $2\theta_{\text{asym}_1}$ to $2\theta_{\text{asym}_6}$ of the measured asymmetric reflections, taking into account the refractive correction.
3. We presume the average interplanar distance d_{av} as the average of the values from d_1 to d_6 .
4. We take the initial values of the parameters a and b based on the parameters c and d_{av} :

$$a_0 = b_0 = \frac{2d_{av}c}{(c^2 - 16d_{av}^2)^{0.5}}$$
The initial values of the other parameters are: $\alpha_0 = \beta_0 = 90^\circ$,
 $\gamma_0 = 120^\circ$.
5. We variate all the parameters a , b , α , β and γ simultaneously in certain ranges with certain steps around the initial values. Strictly speaking, we variate the a and b parameters in the range of 0.04 \AA with a step of 0.01 \AA , the α and β parameters in the range of 0.28° with a step of 0.07° , the γ parameter in the range of 0.4° with a step of 0.1° . For each specific set of parameters, we calculate the interplanar distances for the listed asymmetric reflections, obtaining a set of six values of d_{theoret_i} . We choose the set for which the value: $\sum_{i=1}^6 (d_i - d_{\text{theoret}_i})^2$ is the smallest.
6. We replace the initial values of parameters with the selected set of parameters obtained in the previous step and then we repeat the step 5 with decreasing the variation ranges and the steps twice. We perform 16 iterations.

A convenient way of the presentation of the lattice deformation is the tilt τ of the \mathbf{c} -axis with respect to the normal to the \mathbf{c} -plane and its direction ($\text{dir}\tau$) (Fig. S1). With the fully defined InGaN lattice, the tilt τ can be calculated from the lattice parameters using geometric relationships.

Both the strain and chemical composition affect the lattice parameters, must be determined together and were found by the next iterative fitting. For simplicity, to calculate the indium

content and the components of the strain tensor of the layer, we neglect the tilt of the c -axis. For small misorientation angles like considered in our work, such assumption results in a very small change in the values of the sought parameters.

We assume the x -axis to be parallel to the a -axis of the unit cell and the x - y plane parallel to the axes a and b . However, in such coordinate system shear strain ε_{xy} is non zero. Then, we searched for the coordinate system x' - y' , rotated around the vertical axis by an angle φ , in which the shear strain $\varepsilon_{x'y'}$ is equal to zero ($\varepsilon_{x'y'}=0$), i.e., the principal coordinate system. It is crucial, otherwise, the degree of relaxation calculated with ε_{xx} and ε_{yy} components would be underestimated.

To find the angle of rotation φ , first, we define the components of the strain tensor in the x - y plane of the original coordinate system. We assume that the non-strained (free standing) unit cell has parameter a equal a_0 and its a -axis is parallel to the x -axis and to the a -axis of the strained cell (measured one). (The value of the parameter a_0 is not crucial since it is reduced in the final formula and does not affect the value of φ .) The formulas for the coordinates of the both axes follow:

$$\mathbf{a}_0=(a_0, 0); \mathbf{b}_0=\left\{-\frac{1}{2}a_0, \frac{\sqrt{3}}{2}a_0\right\} \text{ (free standing lattice)}$$

$$\mathbf{a}=(a, 0); \mathbf{b}=(b \cos \gamma, b \sin \gamma) \text{ (strained lattice – partially relaxed)}$$

Versors of the x and y axes are $\mathbf{e}_x=(1, 0)$ and $\mathbf{e}_y=(0, 1)$, respectively. Then \mathbf{a}_0 and \mathbf{b}_0 can be written as:

$$\mathbf{a}_0 = a_0 \mathbf{e}_x; \mathbf{b}_0 = a_0 \left(-\frac{1}{2} \mathbf{e}_x + \frac{\sqrt{3}}{2} \mathbf{e}_y\right)$$

In the strained case, versors \mathbf{e}_x and \mathbf{e}_y transform to vectors \mathbf{e}_{xs} and \mathbf{e}_{ys} while \mathbf{a} and \mathbf{b} axes remain the same function of these vectors:

$$\mathbf{a} = a_0 \mathbf{e}_{xs}; \mathbf{b} = a_0 \left(-\frac{1}{2} \mathbf{e}_{xs} + \frac{\sqrt{3}}{2} \mathbf{e}_{ys}\right)$$

It follows that:

$$\mathbf{e}_{xs} = \frac{\mathbf{a}}{a_0}; \mathbf{e}_{ys} = \frac{1}{\sqrt{3}} \left(2\frac{\mathbf{b}}{a_0} + \frac{\mathbf{a}}{a_0}\right)$$

From elasticity theory:

$$\varepsilon_{xx} = e_{xs_x} - 1;$$

$$\varepsilon_{yy} = e_{ys_y} - 1;$$

$$\varepsilon_{xy} = \varepsilon_{yx} = \frac{1}{2} (e_{xs_y} + e_{ys_x});$$

where e_{xs_x} and e_{ys_y} are corresponding x and y components of the e_{xs} and e_{ys} vectors.

After transformations, we obtain:

$$\varepsilon_{xx} = \frac{a}{a_0} - 1; \varepsilon_{yy} = 2b \sin \gamma / (\sqrt{3} a_0) - 1; \varepsilon_{xy} = b \cos \gamma / (\sqrt{3} a_0).$$

Rotation angle of the system (counterclockwise) is expressed by the formula:

$$\tan(2\varphi) = - \frac{2\varepsilon_{xy}}{\varepsilon_{yy} - \varepsilon_{xx}},$$

which, after transformations, yields to:

$$\tan(2\varphi) = \frac{2b \cos \gamma}{\sqrt{3} a - 2b \sin \gamma}.$$

After calculation of the angle φ we proceed the iterative fitting. We simultaneously vary the indium content, $\varepsilon_{x'x'}$ and $\varepsilon_{y'y'}$ strain components in certain ranges with certain steps. For each specific set, we calculate the theoretical cell parameters in the following steps:

1. We calculate $\varepsilon_{z'z'} = - [C_{13}(\text{In})/C_{33}(\text{In})](\varepsilon_{x'x'} + \varepsilon_{y'y'})$, where the elastic constants C_{13} and C_{33} depend on the indium content and were calculated on the base of the Ref. [S. P. Łepkowski and I. Gorczyca, Physical Review B 83, 203201 (2011)]. The bowing parameter was assumed to be an average of the values in uniform and clustered alloys, given in the reference.
2. We take the strain components $\varepsilon_{x'y'} = \varepsilon_{y'x'} = \varepsilon_{x'z'} = \varepsilon_{z'x'} = \varepsilon_{y'z'} = \varepsilon_{z'y'} = 0$.
3. We transform the strain tensor to the original reference system using found φ angle and obtain the ε tensor.
4. For a chosen indium content, we calculate from Vegard's law the parameters a_L^0 and c_L^0 of the unstrained cell taking the values for GaN ($a=3.1893 \text{ \AA}$ and $c=5.1851 \text{ \AA}$) from Ref. [H. Angerer et al., Applied Physics Letters 71, 1504 (1997)] and for InN ($a=3.538 \text{ \AA}$ and $c=5.702 \text{ \AA}$) from Ref [W. Paszkowicz, Powder Diffraction 14, 258 (1999)].
5. We deform such cell according to the ε tensor and obtain the parameters of the deformed cell: a_{theoret} , b_{theoret} , c_{theoret} , γ_{theoret} .

6. We select the set: indium content, $\varepsilon_{x'x'}$ and $\varepsilon_{y'y'}$ for which the minimum value is obtained by the sum: $[(a-a_{teoret})/a_{err}]^2 + [(b-b_{teoret})/b_{err}]^2 + [(c-c_{teoret})/c_{err}]^2 + [(\gamma-\gamma_{teoret})/\gamma_{err}]^2$, where $a_{err}=b_{err}=0.0005 \text{ \AA}$, $c_{err}=0.0004 \text{ \AA}$, $\gamma_{err}=0.01^\circ$ are reciprocal weights, and the parameters a , b , c , γ are the lattice parameters determined previously.

The procedure is repeated for a smaller range of variation and a smaller step size until the lattice parameters are in satisfactory agreement.